






UNSTATIONARY VISCOELASTIC MHD FLOW OF WALTERS-B LIQUID THROUGH A VERTICAL POROUS PLATE WITH CHEMICAL REACTIONS

 Karnati Veera Reddy^{a*},  G. Ravindranath Reddy^b,  K. Jhansi Rani^c,
 Ayyalappagari Sreenivasulu^d,  Gudala Balaji Prakash^e

^aDepartment of Mathematics, Guru Nanak Institutions Technical Campus, Ranga Reddy (Dt) -501506, Telangana, India

^bMLR Institute of Technology, Dundigal, Hyderabad -500043, Telangana, India

^cFreshman Engineering Department, Lakireddy Bali Reddy College of Engineering,
 L.B. Reddy Nagar, Mylavaram- 521230, Andhra Pradesh, India

^dDepartment of Engineering Mathematics, Koneru Lakshmaiah Education Foundation
 Green fields, Vaddeswaram, Guntur-522302, Andhra Pradesh, India

^eDepartment of Mathematics, Aditya University, Surampalem-533437 Andhra Pradesh, India

Corresponding Author e-mail: veerareddymcmed@gmail.com

Received September 30, 2024; revised January 4, 2025; accepted April 16, 2025

This study investigates the transient magnetohydrodynamic (MHD) flow of Walter's-B viscoelastic fluid over a vertical porous plate within a porous medium, incorporating the effects of radiation and chemical processes. The nonlinear governing equations for the flow are solved using a closed-loop method, yielding detailed numerical solutions for velocity, temperature, and concentration profiles. The results indicate that velocity decreases with increasing permeability (K), Schmidt number (Sc), radiation parameter (R), and magnetic field strength (M), while it increases with higher Prandtl number (Pr), permeability (K), and time (t). Temperature decreases with increasing radiation but rises with higher Prandtl number and time. Similarly, concentration decreases with higher permeability and Schmidt number but increases with time. Notably, an increase in the Brownian motion parameter enhances heat and momentum transfer, resulting in thicker velocity and thermal boundary layers. This research has practical applications in various fields, including blood oxygenators, chemical reactors, and polymer processing industries. The study's novelty lies in its comprehensive integration of radiation, chemical processes, and MHD effects in analyzing viscoelastic fluid flows – a topic that remains underexplored in the literature. Future research could focus on optimizing MHD Walter's-B viscoelastic flow systems, particularly by examining the effects of magnetic field strength and viscoelastic parameters on flow behavior.

Keywords: MHD; Skin friction; Chemical reaction; Radiation and viscoelastic properties

PACS: 44.20.+b; 47.10.ad; 47.11.Bc; 47.15.Cb; 47.35.Tv; 47.50.-d; 47.55.pb; 47.56.+r; 47.65.-d; 47.70.-n

1. INTRODUCTION

A growing number of mathematicians have recently taken an interest in boundary layer flow due to its applications in studying mass and heat transfer phenomena. This interest is motivated by the wide range of applications in various domains, including blood oxygenators, mixing mechanisms, dissolution processes, milk processing, and polymer processing within manufacturing industries. Non-Newtonian fluids are analyzed using a variety of viscoelastic fluid models, such as the Rivlin-Erickson, Maxwell, Walter's-B, micropolar fluids, and second- and third-grade viscoelastic fluids. The boundary layer problem was initially studied by Sakiadis [1, 2], who assumed a constant velocity for the bounding surface. Applications of the boundary layer deformation problem in absorbent materials include geothermal reservoirs and hydroelectric extraction. Crane [3] provided a solution for Newtonian fluid flow over an elastic sheet stretched proportionally to its distance from the origin. Soundalgekar and Wavre [4] investigated unstable free mass transfer and convection through infinite vertical porous plates in a vacuum. Ramana et al. [5] analyzed unsteady free Casson fluid transmission over a semi-infinite vertical porous plate, considering thermal radiation, Soret and Dufour effects, and MHD numerical solutions. Naga Santoshi et al. [6] analysis of MHD Slip Flow of Upper-Convected Casson and Maxwell Nanofluids Over a Porous Stretched Sheet: Effects on Heat and Mass Transfer. Hiremath and Patil [7] studied the effects of free displacement in oscillatory flow through a permeable medium with horizontal and vertical boundaries controlling temperature. Subhashini et al. [8] evaluated the effect of diffusion on flow through a vertical porous plate. Veera et al. [9] examined the impact of thermal radiation and viscous dissipation on Cattaneo–Christov heat flux models for electrically conducting Casson-Carreau nanofluid flows. Nandhini et al. [10] analysed Effect of chemical reaction and radiation absorption on MHD Casson fluid over an exponentially stretching sheet with slip conditions: ethanol as solvent. Nield and Bejan [11] provided a comprehensive review of heat transfer in porous media. Sajid and Hayat [12] applied the homotopy analysis method to investigate the effects of radiation on mixed convection flow over an exponentially stretched sheet. Dash et al. [13] examined unsteady free convection magnetohydrodynamic (MHD) flow in porous media of rotating systems, particularly focusing on pulsating heat and mass transfer while ignoring MHD effects. Subsequently, Irshad et al. [14] studied natural convection simulation of Prabhakar-like fractional Maxwell fluid flowing on inclined plane with generalized thermal flux. Anwar Beg et al. [15] found

computational solutions for free convection at the interface, incorporating the Dufour and Soret effects. This study investigates the numerical behavior of MHD Casson fluid flow with variable properties over an inclined porous stretching sheet, emphasizing the impact of MHD effects on non-Newtonian Casson fluid flow. The analysis employs the Cattaneo–Christov heat flux model to study heat and mass transport in a Casson nanofluid over an accelerating penetrable plate while also examining the effects of thermal radiation on fluid flow dynamics [16–22]. We investigated the magnetohydrodynamic (MHD) numerical solutions for Casson fluid flow over inclined porous elongated sheets with varying properties. Additionally, the research paper "Radiation and Dufour Effects in Unsteady Magnetohydrodynamic Mixed Convective Flow Over an Accelerating Vertical Wavy Plate with Variable Temperature and Mass Diffusion" has made a significant contribution to this field. Abobasari et al. [23] analyzed the entropy generation in unsteady MHD flow over permeable elastic surfaces in nanofluids. Karnati and GVRR [24] Analyses of the Impact of Melting on MHD Casson Fluid Flow Past a Stretching Sheet in a Porous Medium with Radiation. Benazir et al. [25] examined the instability of MHD Casson fluids in vertical cones and plates, considering the effects of inhomogeneous heat sources and sinks. Reddy et al. [26] investigated the melting effects of MHD Casson fluid flow over a long plate in porous media, incorporating electrical effects. G. V. R. et al. [27] analyzed the Soret-Dufour mechanisms and thermal radiation effects on magnetized SWCNT/MWCNT nanofluid in convective transport and solutal stratification. Reddy et al. [28] studied heat and mass transfer in MHD flow of SWCNT and graphene nanoparticle suspensions in Casson fluid. Karnati et al. [29] analyzed unsteady MHD Walter's-B viscoelastic flow past a vertical porous plate. Yaragani et al. [30] examined heat and mass transfer effects on MHD mixed convective flow over a vertical porous surface in the presence of Ohmic heating and viscous dissipation. Gurrampati [31] investigated thermal radiation effects on MHD Casson and Maxwell nanofluids over a porous stretching surface. Devi and Srinivas [32] studied the two-layered immiscible flow of a viscoelastic liquid in a vertical porous channel, considering the Hall current, thermal radiation, and chemical reactions. This study focuses on the kinetics of unsteady magnetohydrodynamic Walter's-B viscoelastic flow over a vertically porous plate within a porous medium, incorporating the effects of radiation and chemical processes. By employing closed analytical techniques, the dimensionless partial differential equations governing the flow field are solved. Numerical solutions facilitate a comprehensive analysis of the velocity, temperature, and concentration profiles, which are examined both qualitatively and graphically to provide deeper insights into the system's behavior. One of the primary gaps in existing research is the interplay between radiation, chemical processes, and MHD Walter's-B viscoelastic flow in porous media. While viscoelastic fluids and MHD flows have been studied independently, their combined effects, particularly under the influence of radiation and chemical interactions, have received limited attention. This work addresses this gap by providing a detailed analysis of flow dynamics over a vertically porous plate. The study solves the dimensionless partial differential equations driving the system using closed analytical methods, aiming to enhance the understanding of temperature, velocity, and concentration profiles and their influence on flow behavior.

2. PROBLEM STATEMENT AND BASIC EQUATIONS

A fluid exhibiting viscoelastic characteristics, which is incompressible and capable of conducting electricity, is moving within an unstable magnetohydrodynamic environment. The flow of a Casson fluid over an infinitely tall vertical porous plate, which starts abruptly, undergoes changes in temperature and mass diffusion while being influenced by thermal radiation. The plate is surrounded by porous media with the X-axis directed towards the plate and the Y-axis perpendicular.

At outset, the fluid and plate have same concentration, denoted as C_m , and temperature T_m . The plate begins moving in the X-direction at time t is zero, with a constant velocity U_0 . A transverse magnetic induction B_0 - applied upright to the direction of flow. Due to the small magnetic Reynolds number and the characteristics of the transverse magnetic field, the induced magnetic fields are deemed insignificant. The concentration of the fluid decreases exponentially, considering a first-order chemical reaction. Because the system extends infinitely in the other direction, the flow variables depend solely on x and y (34).

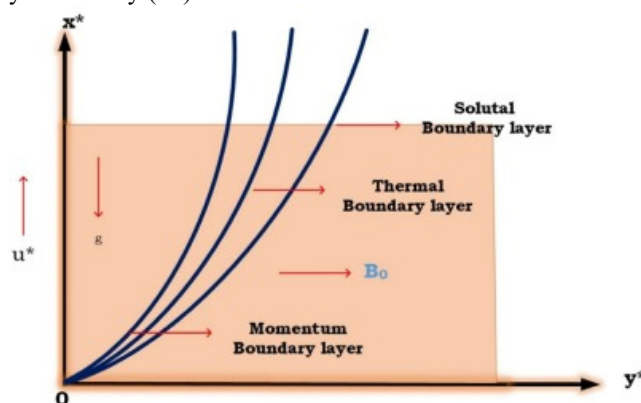


Figure A. Flow geometry of the model

The characteristics of the Casson fluid are:

$$\tau_{ij} = \begin{cases} 2 \left(\mu_B^* + \frac{p_y}{\sqrt{2\pi}} \right) e_{ij}, & \pi > \pi_c \\ 2 \left(\mu_B^* + \frac{p_y}{\sqrt{2\pi_c}} \right) e_{ij}, & \pi < \pi_c \end{cases} \quad (1)$$

Where $\mu_B^*, \pi = e_{ij}e_{ij}$, e_{ij}, π, π_c, p_y be the Non-Newtonian fluid dynamic viscosity, the rate of deformation at the $(i, j)^{th}$ component, The yield stress of the fluid, the critical value of π , and the rate of deformation are considered as separate components.

The governing equations for the boundary layer, taking into account Boussinesq's approximation and the assumptions indicated above, can be expressed as follows (33):

Equation of continuity:

$$\frac{\partial v^*}{\partial y^*} = 0 \Rightarrow v^* = -v_0 \text{ (constant)}. \quad (2)$$

Equation of momentum:

$$\frac{\partial u^*}{\partial t^*} + v^* \frac{\partial u^*}{\partial y^*} = \left[\nu \left(1 + \frac{1}{\beta} \right) \frac{\partial^2 u^*}{\partial y^{*2}} - \lambda \frac{\partial^3 u^*}{\partial y^{*2} \partial t^*} + g \beta_r (T - T_\infty) \cos \alpha \right] + g \beta_c (C - C_\infty) \cos \alpha - \frac{\sigma B_0^2 u^*}{\rho} - \frac{\nu u^*}{K^*} \quad (3)$$

Energy formula:

$$\rho C_p \left(\frac{\partial T}{\partial t^*} + v^* \frac{\partial T}{\partial y^*} \right) = k \frac{\partial^2 T}{\partial y^{*2}} - \frac{\partial q_r}{\partial y^*}. \quad (4)$$

Equation of mass transfer continuity:

$$\frac{\partial C}{\partial t^*} + v^* \frac{\partial C}{\partial y^*} = D \frac{\partial^2 C}{\partial y^{*2}} - k_r (C - C_\infty) + \frac{D_r}{T_\infty} \frac{\partial^2 T}{\partial y^{*2}}, \quad (5)$$

where the coefficient of mass transfer is β_c , the volumetric coefficient of thermal expansion is β_r , the Casson fluid parameter is β , and the gravitational acceleration is represented by g .

This equation ρ describes the relationship between several variables, including fluid density (D), magnetic induction (B_0), radiative heat flow (q_r) in the y -direction, mass diffusion coefficient (D), constant chemical reaction rate (Kr), and porous medium permeability (K^*). The fluid's electrical conductivity is denoted by Sigma. " T " stands for the temperature in dimensions. The specific temperature at constant pressure is shown accordingly as C_p . thermal conductivity of liquids as k , and the viscoelasticity parameter as λ Walter's-B.

The suitable limits to the boundary include

$$\begin{cases} t^* \leq 0 & u^* = 0, T = T_\infty, C = C_\infty \quad \forall y^* \\ t^* > 0 & u^* = u_0, v^* = -v_0, T = T_\infty + (T_w - T_\infty) e^{At^*} \\ & C = C_\infty + (C_w - C_\infty) e^{At^*} \quad \text{At } y^* = 0 \\ & u^* = 0, T \rightarrow \infty, C \rightarrow \infty, \quad y^* \rightarrow \infty, \end{cases} \quad (6)$$

where, $A = \frac{v_0^2}{\nu}$, T_w and C_w are respectively, the place's concentration and temperature.

The radiative heat flux q_r , by using the Rosseland approximation for radiation, can be written as (Alao et al. [33]):

$$q_r = -\frac{4\sigma}{3k_m} \frac{\partial T^4}{\partial y^*} \quad (7)$$

where k_m and σ stand for a constant absorbance coefficient and the Stefan Boltzmann equation, respectively. It is considered that T^{*4} the temperature contrast in the flow is small adequately that it can be expressed as a function of temperature, by neglecting the higher order terms and expansions in the Taylor series about T_∞^* .

$$T^4 \cong 4T_\infty^3 T - 3T_\infty^4 \quad (8)$$

Using equations (7) and (8) in (4), we get

$$\frac{\partial T}{\partial t^*} + v^* \frac{\partial T}{\partial y^*} = \frac{k}{\rho C_p} \frac{\partial^2 T}{\partial y^{*2}} + \frac{16\sigma T_\infty^2}{3k_1 \rho C_p} \frac{\partial^2 T}{\partial y^{*2}} \quad (9)$$

To obtain a dimensionless equation, the following dimensionless quantities must be included:

$$\left\{ \begin{aligned} u &= \frac{u^*}{u_0}, y = \frac{y^* v_0}{v}, t = \frac{t^* v_0^2}{v}, \theta = \frac{T - T_\infty}{T_w - T_\infty}, C = \frac{C - C_\infty}{C_w - C_\infty}, \\ M &= \frac{\sigma B_0^2 v}{\rho v_0^2}, K = \frac{v_0^2 K^*}{v^2}, \text{Pr} = \frac{\rho C_p}{k}, \Gamma = \frac{\lambda v_0^2}{v^2}, Gm = \frac{v g \beta^* (C_w - C_\infty)}{u_0 v_0^2}, Gr = \frac{v g \beta (T_w - T_\infty)}{u_0 v_0^2}, \\ Kr &= \frac{k_r v}{v_0^2}, R = \frac{4\sigma T_\infty^3}{k_1 k}, Sc = \frac{v}{D} \end{aligned} \right. \quad (10)$$

Magnetic term(M), Thermal Grashof(Gr), Mass Grashof(Gm), Permability(K), Radiation term(R), Prandtl(Pr), viscoelastic parameters (Γ), Brownian motion term(Nb), Thermophoresis term(Nt), Schmidt (Sc), Chemical reaction (Kr). The engineering quantities of interest are Sherwood number(Sh), Skin friction coefficient (C_f) and Nussell number (Nu).

The non-dimensional forms of equations (3), (4), and (9) are obtained by virtue of equation (10).

$$\frac{\partial u}{\partial t} - \frac{\partial u}{\partial y} = \left(1 + \frac{1}{\beta}\right) \frac{\partial^2 u}{\partial y^2} - \Gamma \frac{\partial^3 u}{\partial y^2 \partial t} + Gr\theta + GmC - \left(M + \frac{1}{K}\right)u \quad (11)$$

$$\frac{\partial \theta}{\partial t} - \frac{\partial \theta}{\partial y} = \frac{1}{\text{Pr}} \left(1 + \frac{4R}{3}\right) \frac{\partial^2 \theta}{\partial y^2} \quad (12)$$

$$\frac{\partial C}{\partial t} - \frac{\partial C}{\partial y} = \frac{1}{Sc} \frac{\partial^2 C}{\partial y^2} - KrC + \frac{Nt}{Nb} \frac{\partial^2 T}{\partial y^2} = 0 \quad (13)$$

In non-dimensional form, the appropriate beginning and boundary conditions are:

$$\left\{ \begin{aligned} t \leq 0 \quad & u = 0, \theta = 0, C = 0 \quad \forall y \\ t > 0 \quad & u = 1, \theta = e^t, C = e^t \quad \text{at } y = 0 \\ & u = 0, u \rightarrow 0, C \rightarrow 0, y \rightarrow \infty \end{aligned} \right. \quad (14)$$

Solution of the problem

To simplify the operation of the partial deferential equation given above, We can use the inequality to express the speed, temperature as follows:

$$u(y, t) = u_0(y) e^{i\omega t} \quad (15)$$

$$\theta(y, t) = \theta_0(y) e^{i\omega t} \quad (16)$$

$$C(y, t) = C_0(y) e^{i\omega t} \quad (17)$$

Definitions and Physical Interpretations

	Definition	Unit	Complex Nature	Physical Interpretation
u(y, t) (Velocity Profile)	Represents the fluid velocity at a given position y and time t.	m/s (meters per second).	Generally a complex quantity due to the exponential term involving i. The real part u represents the physical velocity.	Describes how the velocity of the fluid varies both in the spatial (y) and temporal (t) dimensions.
u₀(y) (Amplitude of Velocity Profile)	Represents the spatially dependent amplitude of the velocity	m/s.	Can be real or complex, depending on the problem context.	Describes the variation of the velocity amplitude as a function of position y, without considering time dependence.
θ(y,t)	Represents the temperature field or another scalar field (such as concentration) as a function of space (y) and time (t).	Depends on the physical quantity; for temperature, it's typically Kelvin (K) or Celsius (°C).	Complex quantity due to the exponential term.	Describes how the field (temperature, concentration, etc.) varies in space and time, with oscillatory behavior introduced by the term.
θ₀(y)	Represents the amplitude of the field as a function of the spatial coordinate y.	Depends on the physical quantity; for temperature, it's typically Kelvin (K) or Celsius (°C).	It can be complex if the system introduces phase shifts spatially.	Defines the spatial variation of the field's amplitude, serving as the base profile modulated by time.
C(y, t) (Concentration or Property of Interest)	Represents the quantity of interest (e.g., chemical concentration, temperature, or similar scalar property) as a function of spatial coordinate y and time t.	Depends on the context (e.g., mol/m ³ for concentration).	This is a complex quantity because it involves, which introduces a complex phase.	Describes the variation of the property over space and time. The imaginary part (if considered) can represent oscillatory components such as wave behavior.
C₀ (Amplitude Function)	Represents the spatially dependent amplitude or initial distribution of the property CC at t=0.	Depends on the context (e.g., mol/m ³ for concentration).	Real or complex, depending on whether the initial distribution has a phase component.	Provides the baseline or initial profile of the property in the spatial domain y.
e^{iωt} (Exponential Oscillatory Term)	Exponential term representing the oscillatory nature of the field with time, where ii is the imaginary unit (i ² =-1).	Dimensionless.	Complex quantity, as it includes both real and imaginary parts when expanded: e ^{iωt} =cos(ωt)+isin(ωt).	Describes periodic temporal behavior, with ω as the angular frequency of oscillation.
ω (Angular Frequency)	The angular frequency of the oscillations, representing how quickly the velocity oscillates with time.	rad/s (radians per second).	Real.	Determines the rate of oscillation in the flow. A higher ω implies more rapid oscillations.
y (Spatial Coordinate)	The spatial coordinate perpendicular to the flow direction, where the velocity is evaluated.	meters.	Real.	Describes the position within the flow field where the velocity is measured.
t (Time)	Represents the temporal evolution of the system.	sec.	Real.	Tracks the progression of oscillations or flow changes over time.

We get the following by replacing Eqns (15), (16), and (17) in Eqns (11), (12), and (13).

$$\left(1 + \frac{1}{\beta} - i\omega\Gamma\right) u''_0 + u'_0 - k_3 u_0 + [Gr\theta_0 + GmC_0] \cos \alpha = 0 \quad (18)$$

$$k_1 \theta''_0 + \theta'_0 - i\omega\theta_0 = 0 \quad (19)$$

$$C_0'' + ScC_0' - (Kr + i\omega)C_0 + \frac{Nt}{Nb}\theta_0'' = 0 \quad (20)$$

In this case, the primes signify the differential about Y - axis.

The equivalent conditions are expressed as:

$$\begin{cases} t \leq 0, u_0 = 0, \theta_0 = 0, C_0 = 0 & \forall y \\ t > 0, u_0 = e^{-i\omega t}, \theta_0 = e^{(1-i\omega)t}, C_0 = e^{(1-i\omega)t} & \text{at } y = 0 \\ t > 0, u_0 \rightarrow 0, \theta_0 \rightarrow 0, \phi_0 \rightarrow 0 & \text{as } y \rightarrow \infty \end{cases} \quad (21)$$

Equations (18) to (20) contain the parameters leading to the boundary (21) and are given by:

$$u_0(y) = \left((1 - (A_1 + A_2)e^t) e^{-m_3 y} + (A_1 e^{-m_3 y} + A_2 e^{-m_1 y}) e^{(1-i\omega)t} \right) \quad (22)$$

$$\theta_0(y) = e^{(1-i\omega)t - m_3 y} \quad (23)$$

$$C_0(y) = e^{(1-i\omega)t - m_1 y} \quad (24)$$

Given the aforementioned solutions, the boundary layer's Velocity, Temperature, and Concentration distributions become

$$u(y, t) = \left[(1 - (A_1 + A_2)e^t) e^{-m_3 y} + (A_1 e^{-m_3 y} + A_2 e^{-m_1 y}) e^t \right] \quad (25)$$

$$\theta(y, t) = e^{(t - m_3 y)} \quad (26)$$

$$C(y, t) = e^{(t - m_1 y)} \quad (27)$$

Mass flux, local surface heat transfer, and local wall shear stress are three critical physical parameters, and accurately computing them has become increasingly important. Local wall shear stress, commonly referred to as skin friction, can be determined from the velocity field within the boundary layer. which is currently known as by

$$C_f = \left(\frac{\partial u}{\partial y} \right)_{y=0} = \left[((A_1 + A_2)e^t - 1)m_3 - (m_3 A_1 + m_1 A_2)e^t \right]$$

Following this, we have a look at the non-dimensional expression of the heat transfer rate from the temperature field:

$$Nu = - \left(\frac{\partial \theta}{\partial y} \right)_{y=0} = m_3 e^t$$

Now, we will analyse the rate at which heat is transferred from the temperature field. This rate is expressed in a non-dimensional, as seen below:

$$Sh = - \left(\frac{\partial C}{\partial y} \right)_{y=0} = m_1 e^t$$

RESULTS AND DISCUSSION

This work investigates the interplay of electrical and chemical interactions in studying the MHD Walter's-B viscoelastic instability in vertical voids within porous media. The solutions are analysed based on parameters such as concentration, velocity, and temperature, while other parameters are held constant. The results are presented in Figures 1 to 15, illustrating the effects of various parameters on wall velocity, temperature, and concentration distributions. We considered flow over an infinite vertical plate of finite length. Consequently, the problem is solved within a finite boundary. In the graphical analysis, the y-axis ranges from 0 to 4, and as y approaches 5, the concentration, temperature, and velocity values asymptotically approach zero. This validates the consideration of finite length for the analysis. The study utilizes the following default parameter values: $Gm=3.0$, $Gr=3$, $K=0$, $R=2$, $Pr=0$, $t=0$, $Sc=0$, $\omega=1$, and $M=5$. Additionally, we incorporated inclination, radiation, time and temperature parameters into the analysis.

The results, summarized in the figures, provide a comprehensive understanding of how various factors influence the temperature, velocity, and concentration distributions in MHD Walter's-B viscoelastic flow. A detailed analysis is as follows from figures. Figures 1 and 2: These figures show the effects of media and concentration distributions under the influence of external factors. Both curves decrease with increasing antibody concentration, highlighting the significant role of antibodies in mediating the flow.

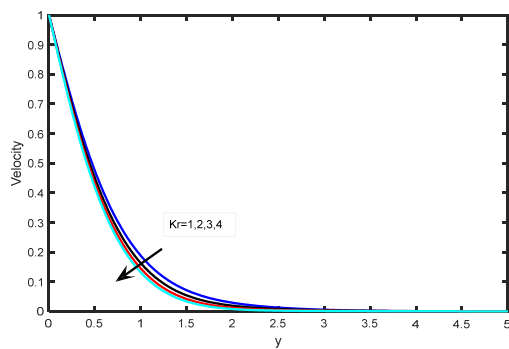


Figure 1. Speed outline for numerous Kr values

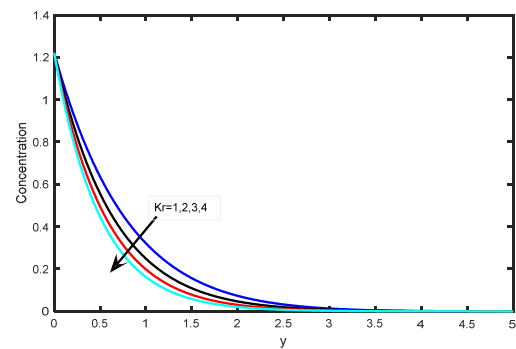


Figure 2. Contour of concentration for varying Kr values

Figure 3: This figure illustrates the impact of the Schmidt number (Sc) on the concentration distribution. Figure 4: It demonstrates how the Schmidt number affects buoyancy-driven flow. As the Schmidt number increases, the concentration buoyancy decreases, leading to reduced velocity and concentration profiles. Figures 5 and 6: These figures depict the temperature profiles under different electric field strengths. Thermal energy coupling increases, causing a reduction in temperature and velocity near the thermal boundary layer.

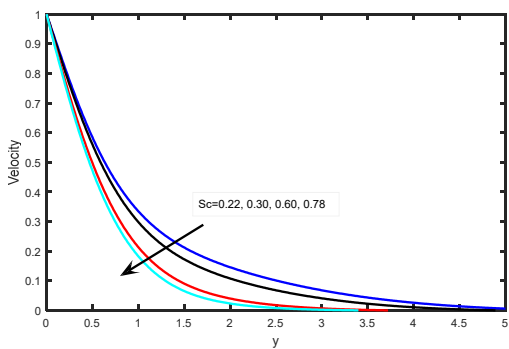


Figure 3. Profiles of Velocity for various Sc values

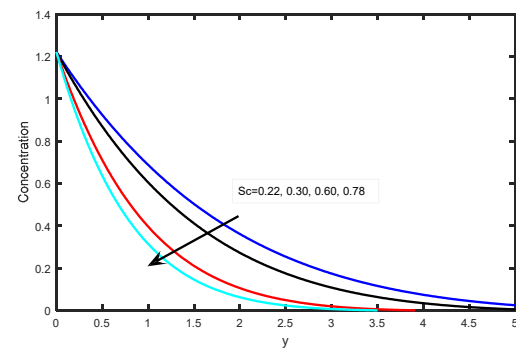


Figure 4. Profiles of concentration for various Schmidt numbers (Sc)

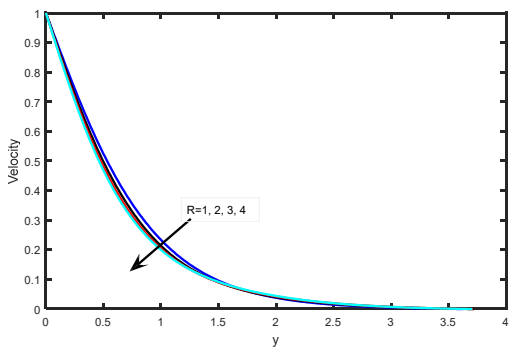


Figure 5. Velocity profiles with various R values

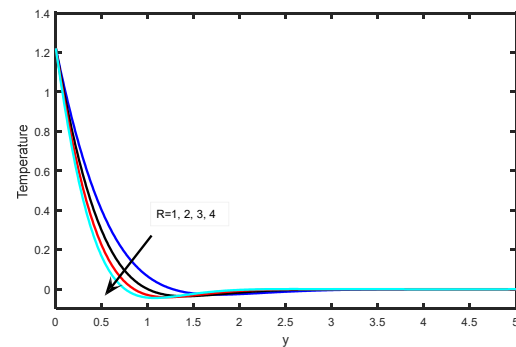


Figure 6. Temperature form with varying R values

Figures 7 and 8: These figures reveal the influence of the Prandtl number (Pr) on temperature and velocity distributions, respectively. Higher Pr values lead to a reduction in flow velocity and thermal diffusion rates.

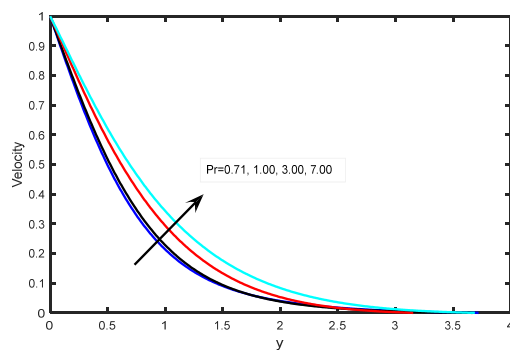


Figure 7. Speed profiles for various Pr values

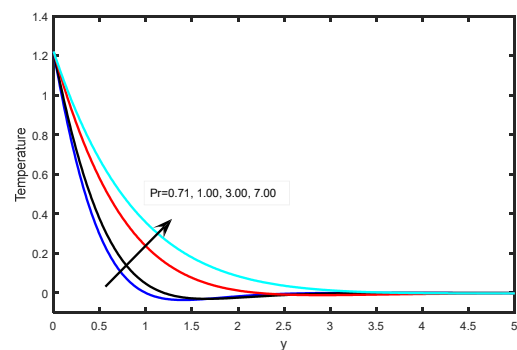


Figure 8. Temperature profiles for various Pr values

Figure 9: This figure highlights the effect of increasing viscoelastic parameters (Γ) on velocity distribution, resulting in a flatter velocity profile. Figure 10: This figure examines the effect of permeability (K) on flow. Increased permeability enhances the velocity of the boundary layer while reducing the resistance within the porous medium.

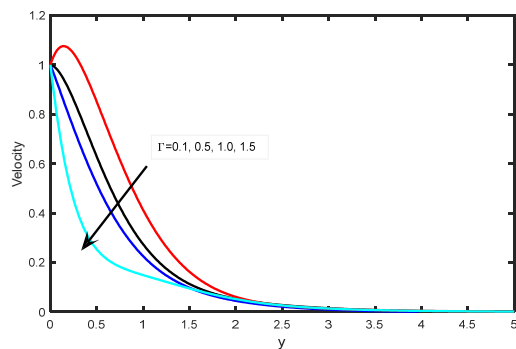


Figure 9. Velocity profiles with varying Γ values

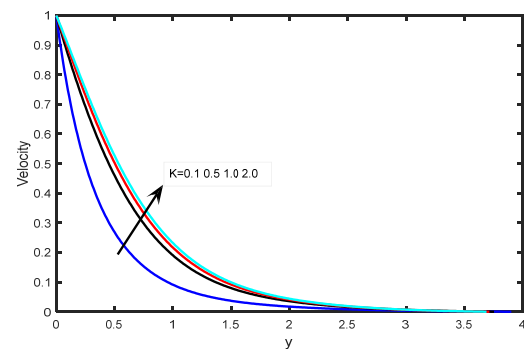


Figure 10. Velocity profiles with varying K

Figure 11: It shows the impact of the magnetic field strength (M) on velocity. A stronger magnetic field reduces velocity due to increased electromagnetic damping. Figures 12, 13, and 14: These figures illustrate the influence of time (t) on concentration, velocity, and temperature profiles, respectively. All three profiles increase over time, reflecting the system's evolving behaviour.

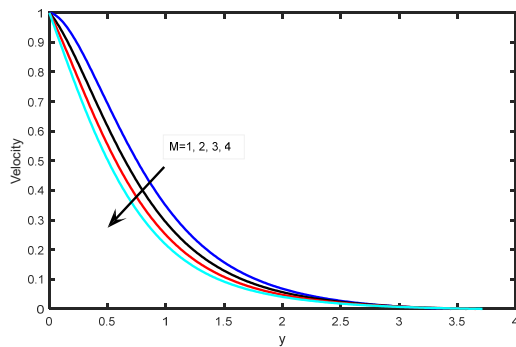


Figure 11. Velocity profiles for various M values

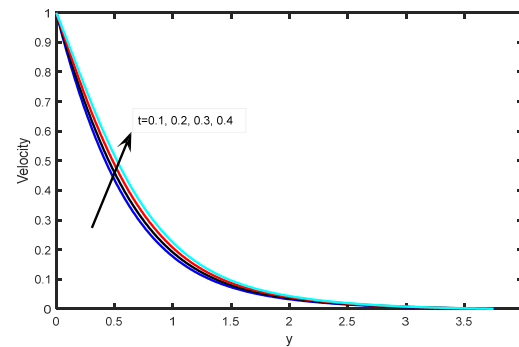


Figure 12. Velocity profiles for various time (t) values

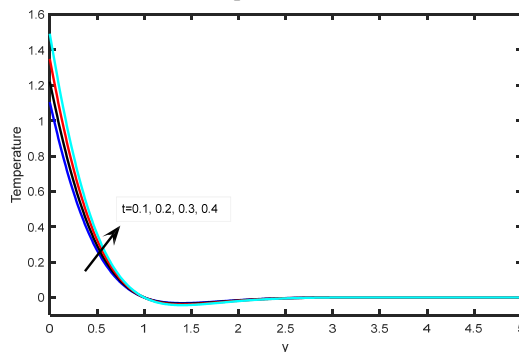


Figure 13. Temperature profiles over various time intervals (t)

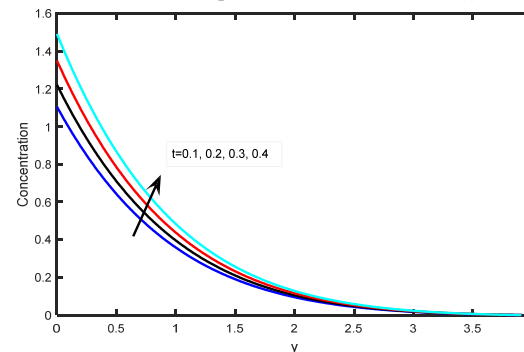


Figure 14. Profiles of concentration for various time values (t)

CONCLUSIONS

This study provides a comprehensive numerical simulation of viscoelastic magneto hydrodynamic (MHD) flow along a vertical plate, using the Walter's-B model to analyze the influence of electrical and chemical interactions. The results are interpreted from a physical perspective, offering insights with potential engineering applications. Key findings include:

➤ Velocity Dynamics:

- **Decrease in Velocity:** The velocity of the fluid decreases with increasing values of the chemical reaction parameter (K_r), Schmidt number (Sc), radiation parameter (R), and magnetic field parameter (M). This implies that higher chemical reaction rates, stronger magnetic fields, or greater diffusivity of the solute reduce fluid motion. Engineering systems can exploit these effects to regulate flow speed in applications such as chemical reactors and cooling systems.
- **Increase in Velocity:** Velocity increases with higher values of the Prandtl number (Pr), permeability parameter (K), and time (t). These results highlight the potential to enhance flow velocity by modifying thermal properties or adjusting permeability in porous materials, which is critical in optimizing filtration systems and thermal insulation designs.

➤ **Temperature Behavior:**

- **Decrease in Temperature:** The temperature decreases as the radiation parameter (R) rises, suggesting that stronger radiative heat transfer dissipates thermal energy effectively. This is beneficial in applications like radiative cooling technologies.
- **Increase in Temperature:** An increase in the Prandtl number (Pr) and time (t) leads to a rise in temperature. This highlights the importance of thermal diffusivity and time-dependent heat transfer in systems requiring precise thermal regulation.

➤ **Concentration Variations:**

- **Decrease in Concentration:** Concentration levels decrease with higher values of the chemical reaction parameter (Kr) and Schmidt number (Sc). These findings can be leveraged to control solute transport in processes such as pollutant dispersion or chemical separation.
- **Increase in Concentration:** Concentration increases with time (t), emphasizing the role of prolonged processes in enhancing solute distribution, relevant for long-duration mixing or diffusion-controlled reactions.
- **Impact of Brownian Motion:** An increase in the Brownian motion parameter enhances both temperature and velocity profiles, improving heat and momentum transfer. This effect also thickens the velocity and thermal boundary layers, which is advantageous for applications requiring enhanced energy dissipation or thermal buffering.

Engineering Applications: These findings have significant implications for optimizing industrial systems involving MHD viscoelastic flows, such as:

- **Heat and Mass Transfer Systems:** Understanding the interplay between parameters like Pr , Sc , and R allows for better design of heat exchangers and chemical reactors.
- **Magnetically Controlled Flows:** The effect of the magnetic field parameter (M) on velocity provides a pathway to tailor flow profiles in electromagnetic pumps and magnetic drug delivery systems.
- **Filtration and Separation Technologies:** Insights into the concentration dynamics under varying Sc and Kr values can improve the efficiency of separation processes in chemical engineering.
- **Thermal Insulation and Cooling:** Leveraging radiative heat transfer (R) effects can enhance the performance of cooling and insulation systems.

Future Directions: Future studies could delve into the relationship between antibody concentration and other fluid dynamics parameters, especially in the context of heat and mass transfer rates. Additionally, exploring the effects of varying magnetic field intensities and viscoelastic parameters on complex flow patterns may provide deeper insights into optimizing MHD Walter's-B viscoelastic flow systems for practical engineering applications.

Nomenclature

g	Acceleration due to gravity (unit: $m \cdot s^{-2}$)
Kr	Dimensional chemical reaction component
C	Fluid concentration (unit: $kg \cdot m^{-3}$)
T	Fluid temperature (unit: K)
D	Mass diffusivity (unit: $m^2 \cdot s^{-1}$)
C_p	Specific heat at constant pressure (unit: $J \cdot kg^{-1} K^{-1}$)
u^*	Velocity component along x^* (unit: $m \cdot s^{-1}$)
Greek symbols	
ρ	Density at a distance from the plate (unit: $kg \cdot m^{-3}$)
θ	Dimensionless fluid temperature
ϕ	Dimensionless species concentration
ρ	fluid density (unit: $kg \cdot m^{-3}$)
ν	kinematic viscosity (unit: $m^2 \cdot s^{-1}$)
k	Thermal conductivity (unit: $W \cdot m^{-1} \cdot K^{-1}$)
βC	Expansion of concentration coefficient (unit: K^{-1})
βT	Thermal expansion coefficient (unit: K^{-1})

ORCID

- ©Karnati Veera Reddy, <https://orcid.org/0000-0003-1073-7551>;
 ©G. Ravindranath Reddy, <https://orcid.org/0000-0002-3568-8576>
 ©K. Jhansi Rani, <https://orcid.org/0000-0002-2400-6576>;
 ©Ayyalappagari Sreenivasulu, <https://orcid.org/0000-0003-3992-6436>
 ©Gudala Balaji Prakash, <https://orcid.org/0000-0003-1892-4634>

REFERENCES

- [1] B.C. Sakiadis, "Boundary layer behavior on continuous solid surfaces: I. boundary layer equations for two dimensional and axisymmetric flow," *AICHE*, **7**, 26-28 (1961). <https://doi.org/10.1002/aic.690070108>
- [2] B.C. Sakiadis, "Boundary layer behavior on continuous solid surfaces: II. Boundary layer on a continuous flat surface," *AICHE*, **7**, 221-225 (1961). <https://doi.org/10.1002/aic.690070211>
- [3] L.J. Crane, "Flow past a stretching plate," *ZAMP*, **21**, 645-655 (1970). <https://doi.org/10.1007/BF01587695>

- [4] V.M. Soundalgekar, and P.D. Wavre, "Unsteady free convection flow past an infinite vertical plate with constant suction and mass transfer," *Int. J. Heat Mass Transf.* **20**, 1363-1373 (1977). [https://doi.org/10.1016/0017-9310\(77\)90033-3](https://doi.org/10.1016/0017-9310(77)90033-3)
- [5] K.V. Reddy, G.V.R. Reddy, A. Sandhya, and Y.H. Krishna, "Numerical solution of MHD, Soret, Dufour, and thermal radiation contributions on unsteady free convection motion of Casson liquid past a semi-infinite vertical porous plate," *Heat Transfer*, **51**(3), 2837-2858 (2022). <https://doi.org/10.1002/hjt.22452>
- [6] V. Seethamahalakshmi, R. Leelavathi, T.S. Rao, P.N. Santoshi, G.V.R. Reddy, and A.S. Oke, "MHD slip flow of upper-convected Casson and Maxwell nanofluid over a porous stretched sheet: impacts of heat and mass transfer," *CFD Letters*, **16**(3), 96-111 (2024). <https://doi.org/10.37934/cfdl.16.3.96111>
- [7] P.S. Hiremath, and P.M. Patil, "Free convection effects on oscillatory flow of couple stress field through a porous medium," *Acta Mech.* **98**, 143-158 (1993). <https://doi.org/10.1007/BF01174299>
- [8] A. Subhashini, N.R. Bhaskara, C.V.R. Kumari, "Mass transfer effects on the flow past a vertical porous plate," *J. Energy Heat Mass Transf.* **993**(15), 221-226 (1993).
- [9] K.V. Reddy, V.R. Reddy, G., and A.J. Chamkha, "Effects of Viscous Dissipation and Thermal Radiation on an Electrically Conducting Casson-Carreau Nanofluids Flow with Cattaneo-Christov Heat Flux Model," *Journal of Nanofluids*, **11**(2), 214-226 (2022). <https://doi.org/10.1166/jon.2022.1836>
- [10] C.A. Nandhini, S. Jothimani, and A.J. Chamkha, "Effect of chemical reaction and radiation absorption on MHD Casson fluid over an exponentially stretching sheet with slip conditions: ethanol as solvent," *European Physical Journal Plus*, **138**(1), (2023). <https://doi.org/10.1140/epjp/s13360-023-03660-8>
- [11] D.A. Nield, and A. Bejan, *Convection in Porous Media*, 2nd ed. (Springer-Verlag, Berlin 1998). <https://doi.org/10.1007/978-1-4757-3033-3>
- [12] M. Sajid, and T. Hayat, "Influence of thermal radiation on the boundary layer flow due to an exponentially stretching sheet," *Int. Comm. Heat Mass Transf.* **35**, 347-356 (2008). <https://doi.org/10.1016/j.icheatmasstransfer.2007.08.006>
- [13] G.C. Dash, P.K. Rath, and A.K. Patra, "Unsteady free convective MHD flow through porous media in a rotating system with fluctuating temperature and concentration," *Modell. Controll. B*, **78**(3), 1-16 (2009).
- [14] I. Khan, R. Ali, M.A. Shakir, A.S. Al-Johani, A.A. Pasha, and K. Irshad, "Natural convection simulation of Prabhakar-like fractional Maxwell fluid flowing on inclined plane with generalized thermal flux," *Case Studies in Thermal Engineering*, **35**, 102042 (2022). <https://doi.org/10.1016/j.csite.2022.102042>
- [15] O.A. Be'g O, A.Y. Bakier, and V.R. Prasad, "Numerical study of free convection magnetohydrodynamic heat and mass transfer from a stretching surface to a saturated porous medium with Soret and Dufour effects," *Comput. Mater. Sci.* **46**, 57-65 (2009). <https://doi.org/10.1016/j.commatsci.2009.02.004>
- [16] K.V. Reddy, G.V.R. Reddy, A. Akgül, R. Jarrar, H. Shanak, and J. Asad, "Numerical solution of MHD Casson fluid flow with variable properties across an inclined porous stretching sheet," *AIMS Mathematics*, **7**(12), 20524-20542 (2022). <https://doi.org/10.3934/math.20221124>
- [17] K.V. Reddy, G.V.R. Reddy, and Y.H. Krishna, "Effects of Cattaneo-Christov heat flux analysis on heat and mass transport of Casson nano liquid past an accelerating penetrable plate with thermal radiation and Soret-Dufour mechanism," *Heat Transfer*, **50**(4), 3458-3479 (2021). <https://doi.org/10.1002/hjt.22036>
- [18] M.M. Rashidi, E. Momoniat, and B. Rostami, "Analytic approximate solution for MHD boundary layer viscoelastic fluid flow over continuously moving stretching surface by HAM with two auxiliary parameters," *J. Appl. Math.* (2012). <https://doi.org/10.1155/2012/780415>
- [19] R. Sivaraj, and B.R. Kumar, "Unsteady MHD dusty viscoelastic fluid Couette flow in an irregular channel with varying mass diffusion," *Int. J. Heat Mass Transf.* **55**, 3076-3089 (2012). <https://doi.org/10.1016/j.ijheatmasstransfer.2012.01.049>
- [20] T. Poornima, and B.N. Reddy, "Radiation effects on MHD free convective boundary layer flow of nanofluids over a nonlinear stretching sheet," *Adv. Appl. Sci. Res. Pelagia Res.* **4**(201), 190-202 (2013).
- [21] S.R. Mishra, G.C. Dash, and M. Acharya, "Free convective flow of viscoelastic fluid in a vertical channel with DuFour effect," *World Appl. Sci. J.* **28**(9), 1275-1280 (2013).
- [22] J. Prakash, B.R. Kumar, and R. Sivaraj, "Radiation and Dufour effects on unsteady MHD mixed convective flow in an accelerated vertical wavy plate with varying temperature and mass diffusion," *Walailak J. Sci. Technol.* **11**, 939-954 (2013). <https://www.thaiscience.info/Journals/Article/WJST/10958529.pdf>
- [23] M.H. Abolbashari, N. Freidoonimehr, F. Nazari, and M.M. Rashidi, "Entropy analysis for an unsteady MHD flow past a stretching permeable surface in nanofluid," *Powder Technol.* **267**, 256-267 (2014). <https://doi.org/10.1016/j.powtec.2014.07.028>
- [24] K.V. Reddy, and G.V.R. Reddy, "Outlining the impact of melting on mhd casson fluid flow past a stretching sheet in a porous medium with radiation," *Biointerface Research in Applied Chemistry*, **13**, 1-14 (2022). <https://doi.org/10.33263/BRIAC131.042>
- [25] A.J. Benazir, R. Sivraj, and O.D. Makind, "Unsteady MHD Casson fluid flow over a vertical cone and flat plate with non-uniform heat source/sink," *Int. J. Eng. Res. Africa*, **21**, 69-83(2015). <https://doi.org/10.4028/www.scientific.net/JERA.21.69>
- [26] K.V. Reddy, and G.V.R. Reddy, "Outlining the Impact of Melting on MHD Casson Fluid Flow Past a Stretching Sheet in a Porous Medium with Radiation," *Biointerface Research in Applied Chemistry*, **13**, 1-14 (2022). <https://doi.org/10.33263/BRIAC131.042>
- [27] B.O. Falodun, O. Ramakrishna, A.S. Ismail, T.M. Oladipupo, O.T. Idiat, A.I. Oyeyemi, and G.V.R. Reddy, "Soret-Dufour mechanisms and thermal radiation effects on magnetized SWCNT/MWCNT nanofluid in a convective transport and solutal stratification analysis," *Ain Shams Engineering Journal*, **15**(10), 102853 (2024). <https://doi.org/10.1016/j.asej.2024.102853>
- [28] A.S. Oke, B.A. Juma, and G.V.R. Reddy, "Heat and mass transfer in MHD flow of SWCNT and graphene nanoparticles suspension in Casson fluid," *ZAMM-Journal of Applied Mathematics and Mechanics/Zeitschrift für Angewandte Mathematik und Mechanik*, **104**(12), e202300106 (2024). <https://doi.org/10.1002/zamm.202300106>
- [29] V.R. Karnati, S. Akuri, O. Ramakrishna, M. Gayatri, S.R. Tagallamudi, and V.R.R. Gurrampati, "Unsteady MHD Walter's B Viscoelastic Flow Past a Vertical Porous Plate," *CFD Letters*, **16**(12), 85-96 (2024). <https://doi.org/10.37934/cfdl.16.12.8596>
- [30] H.K. Yaragani, A. Anumolu, B. Pathuri, and G.V.R. Reddy, "Heat and Mass Transfer Effects on MHD Mixed Convective Flow of a Vertical Porous Surface in the Presence of Ohmic Heating and Viscous Dissipation," *CFD Letters*, **16**(12), 72-84 (2024). <https://doi.org/10.37934/cfdl.16.12.7284>

- [31] T.S. Rao, M.M. Babu, R.R. Bojja, and V.R.R. Gurrampati, "Thermal radiation effects on mhd casson and maxwell nanofluids over a porous stretching surface," *Passer Journal of Basic and Applied Sciences*, **6**(1), 171-178 (2024). <https://doi.org/10.24271/psr.2024.416203.1389>
- [32] M.P. Devi, and S. Srinivas, "Two layered immiscible flow of viscoelastic liquid in a vertical porous channel with Hall current, thermal radiation and chemical reaction," *International Communications in Heat and Mass Transfer*, **142**, 106612 (2023). <https://doi.org/10.1016/j.icheatmasstransfer.2023.106612>
- [33] F.I. Alao, A.I. Fagbade, and B.O. Falodun, "Effects of thermal radiation, Soret and Dufour on an unsteady heat and mass transfer flow of a chemically reacting fluid past a semi-infinite vertical plate with viscous dissipation," *Journal of the Nigerian Mathematical Society*, **35**, 142–158 (2016). <https://doi.org/10.1016/j.jnnms.2016.01.002>
- [34] Y.D. Reddy, B.S. Goud, and M.A. Kumar, "Radiation and heat absorption effects on an unsteady MHD boundary layer flow along an accelerated infinite vertical plate with ramped plate temperature in the existence of slip condition," *Partial Differential Equations in Applied Mathematics*, **4**, 100166 (2021). <https://doi.org/10.1016/j.padiff.2021.100166>

Appendix

$$u(y, t) = u_0(y)e^{i\omega t}$$

$$\theta(y, t) = \theta_0(y)e^{i\omega t}$$

$$C(y, t) = C_0(y)e^{i\omega t}$$

$$C_0(y) = A_1 e^{-m_1 y} + A_2 e^{-m_2 y}$$

$$\theta_0(y) = A_3 e^{-m_1 y}$$

$$u_0(y) = A_6 e^{-m_3 y} + A_4 e^{-m_1 y} + A_5 e^{-m_2 y}$$

$$k_1 = \frac{1}{Pr} \left(1 + \frac{4R}{3} \right), \quad k_2 = -m_1^2 \left(\frac{Nt}{Nb} \right) e^{(1-i\omega)t},$$

$$k_3 = i\omega + M + \frac{1}{k}, \quad k_4 = \Gamma i\omega$$

$$m_1 = \frac{1 + \sqrt{1 + 4i\omega k_1}}{2}$$

$$m_2 = \frac{Sc + \sqrt{Sc^2 + 4(K_r + i\omega)}}{2}, \quad m_3 = \frac{1 + \sqrt{1 + 4k_3 k_4}}{K_4}$$

$$A_1 = \frac{k_2}{m_1^2 - Scm_1 - (K_r + i\omega)}; \quad A_2 = A_3 - A_1; \quad A_3 = e^{(1-i\omega)t};$$

$$A_4 = \frac{-GrA_3 - GmA_1}{k_4 m_1^2 - m_1 - k_3}; \quad A_5 = \frac{-GmA_2}{k_4 m_2^2 - m_2 - k_3}; \quad A_6 = e^{-i\omega t} - A_4 - A_5$$

НЕСТАЦІОНАРНИЙ В'ЯЗКОПРУЖНИЙ МГД ПОТІК WALTERS-B РІДИНИ ЧЕРЕЗ ВЕРТИКАЛЬНУ ПОРИСТУ ПЛАСТИНУ З ХІМІЧНИМИ РЕАКЦІЯМИ

Карнаті Віра Редді^a, Г. Равіндранат Редді^b, К. Джхансі Рані^c, Айялаппагарі Шрінівасулу^d, Гудала Баладжі Пракаш^e

^aКафедра математики, Технічний кампус Інституту Гуру Нанак, Ранга Редді (Dt) -501506, Телангана, Індія

^bТехнологічний інститут MLR, Дандігал, Хайдерабад -500043, Телангана, Індія

^cКафедра інженерії для першокурсників, Інженерний коледж Лакіредді Балі Редді,

Л.Б. Редді Нагар, Мілаварам - 521230, Андхра-Прадеш, Індія

^dКафедра інженерної математики, Освітній фонд Конеру Лакшмаї,

Грін-Філдс, Ваддесварам, Гунтур - 522302, Андхра-Прадеш, Індія

^eКафедра математики, Університет Адітья, Сурампадем - 533437, Андхра-Прадеш, Індія

У роботі досліджується перехідний магнітогідродинамічний (МГД) потік в'язкопружної рідини Walter's-B над вертикальною пористою пластинною в пористому середовищі, що включає вплив радіації та хімічних процесів. Нелінійні керуючі рівняння для потоку розв'язуються за допомогою методу замкнутого циклу, що дає детальні чисельні рішення для профілів швидкості, температури та концентрації. Результати показують, що швидкість зменшується зі збільшенням проникності (K), числа Шмідта (Sc), параметра випромінювання (R) і напруженості магнітного поля (M), тоді як вона збільшується зі збільшенням числа Прандтля (Pr), проникності (K) і часу (t). Температура знижується зі збільшенням радіації, але підвищується зі збільшенням числа Прандтля та часу. Подібним чином концентрація зменшується з підвищенням проникності та числа Шмідта, але збільшується з часом. Примітно, що збільшення параметра броунівського руху посилює передачу тепла та імпульсу, що призводить до більш товстих швидкісних і теплових прикордонних шарів. Це дослідження має практичне застосування в різних галузях, включаючи оксигенатори крові, хімічні реактори та промисловість переробки полімерів. Новизна дослідження полягає в комплексній інтеграції випромінювання, хімічних процесів і ефектів МГД в аналізі потоків в'язкопружної рідини – теми, яка залишається недостатньо вивченою в літературі. Майбутні дослідження можуть бути зосереджені на оптимізації МГД-в'язкопружних систем Walter's-B потоку, зокрема шляхом вивчення впливу напруженості магнітного поля та в'язкопружних параметрів на поведінку потоку.

Ключові слова: МГД; поверхневе тертя; хімічна реакція; радіаційні та в'язкопружні властивості